Analytical Methods

PAPER

View Article Online
View Journal | View Issue

Cite this: *Anal. Methods*, 2016, **8**, 4197

Fabrication and adsorption characterization of single-walled carbon nanotube (SWNT) buckypaper (BP) for use in air samplers

J. Oh,[a] E. L. Floyd,[b] T. C. Watson[b] and C. T. Lungu*[a]

Received 17th March 2016
Accepted 11th May 2016

DOI: 10.1039/c6ay00783j

www.rsc.org/methods

Single-walled carbon nanotubes (SWNTs) have been investigated as a promising sorbent for volatile organic compound (VOC) sampling. We also successfully demonstrated that pre-analysis desorption can be achieved by irradiating the sorbent with high intensity visible light pulses. This technique, photothermal desorption (PTD), can improve sensitivity and shorten current analytical procedure. Different fabrication methods of a buckypaper (BP), a self-supporting form of carbon nanotubes (CNTs), were explored; three methods using arc discharge (AD) SWNTs included non-cleaned, acetone-cleaned, and methanol-cleaned and one method using high-pressure carbon monoxide (HiPco) SWNTs. Adsorption efficiencies of the fabricated BPs were compared in terms of Brunauer, Emmett, and Teller (BET) surface area, pore size, and toluene adsorption capacity. All materials were found to have high BET surface area (211 to 649 $m^2\ g^{-1}$) and toluene adsorption capacity (25 to 106 mg g^{-1}) but HiPco BP exhibited the highest BET surface area (649 $\pm$ 3 $m^2\ g^{-1}$) with the smallest mean pore size (7.7 $\pm$ 0.3 nm) and the greatest toluene adsorption capacity (106 mg g^{-1}). Additionally, HiPco BP had the simplest fabrication process which taken as a whole is a clear indication that further investigations using the PTD technique should be explored with this material.

Introduction

Passive sampling of volatile organic compounds (VOCs) followed by laboratory analysis either through chemical or thermal extraction has been accepted in the workplace because of the convenience, cost effectiveness, and wearer acceptability of passive samplers over active sampling devices.[1–3] However, passive samplers are generally limited in capability for very low exposure situations or short duration sampling because of their higher limit of detection caused by the relatively slow sampling rate driven by diffusion.[4] Moreover, for industries seeking to demonstrate regulatory compliance, the long time lag between collecting samples and getting results back[5] and expensive laboratory analysis have been a burden. Recently, our group developed a novel analytical technique called photothermal desorption (PTD) which can improve the sensitivity of the analysis of passive samplers and help shorten the current exposure assessment procedure to improve workers' protection by faster turn-around-time for analytical results.[6] In PTD, a pulse of light thermally desorbs analyte collected on a sorbent which releases VOCs. VOCs can be directly measured with a photo-ionization detector (PID) or directed to a gas chromatograph (GC) for detailed analysis. However, further development of a new sorbent which will work efficiently with this new desorption technique is still needed.

In this study, single-walled carbon nanotubes (SWNTs) were evaluated as potential sorbents for PTD because of their efficient light absorption,[7,8] exceptionally high thermal conductivity[9,10] and high Brunauer, Emmett, and Teller (BET) specific surface area.[11] While in general carbon nanotubes (CNTs) have shown promising features for VOC adsorption,[12–14] for passive sampling applications they need to be fabricated into a reusable, sturdy form which will preserve its physical integrity under normal working conditions. The purpose of this study was to examine fabrication methods of SWNTs to obtain BPs that are favorable for use with PTD. To accomplish this we compared their adsorption properties through examining BET surface area, average pore size, and toluene adsorption capacity. Previously, SWNTs synthesized by chemical vapor deposition (CVD) were examined due to their low cost and the scalability of synthesis.[6] However, we were unsuccessful in processing CVD SWNT into a self-supporting form (*i.e.*, buckypaper, BP). Therefore, in this study SWNTs obtained through arc discharge (AD) and high-pressure carbon monoxide (HiPco) syntheses were investigated since we were able to easily process these into BPs in our lab. Additionally, mechanical properties of the fabricated BPs were characterized to examine their physical integrity.

[a]*Department of Environmental Health Sciences, University of Alabama at Birmingham, Birmingham, AL, USA. E-mail: clungu@uab.edu*

[b]*Department of Occupational and Environmental Health, University of Oklahoma, Oklahoma City, OK, USA*

Experimental

Fabrication of buckypapers (BPs)

High purity AD SWNT and HiPco SWNT were purchased from NanoIntegris Inc. (Quebec, Canada). AD SWNT (94.5%) was pre-suspended in a surfactant solution (0.5 mg mL^{-1}, 1% w/v sodium cholate and 1% w/v sodium dodecyl sulfate in water). HiPco SWNT was powder (85%). Vacuum filtration of liquid suspended SWNT was employed to fabricate BPs[15,16] with a cleaning process added to remove potential surfactants from the AD SWNTs based on the manufacturer's recommendations.[17] For the fabrication of AD BPs, 100 mL (50 mg) of the AD SWNT suspension was mixed with 400 mL of acetone for 15 hours (Fig. 1). The suspension was then vacuum-filtered through a polytetrafluoroethylene (PTFE) membrane filter (47 mm diameter, 5 μm pore, EMD Millipore, Darmstadt, Germany) and allowed to dry for approximately 2 hours while on the filter membrane. A BP was obtained by delaminating the dried SWNT cake from the filter (non-cleaned AD BP). For solvent cleaned BPs, a series of two alternating rinses were used, a water rinse then solvent rinse was administered after the SWNT cake was deposited but not dried. The SWNT cake was first rinsed with 250 mL of deionized water (18.2 MΩ cm) then 50 mL of solvent to make either acetone-cleaned or methanol-cleaned AD BP.

For HiPco BP preparation, 50 mg of powdered HiPco SWNTs were suspended in 400 mL methanol and ultra-sonicated using a 490 W bath sonicator (BRANSON CPX5800H, Danbury, CT) for 90 minutes. The solution was vacuum-filtered through the same type PTFE membrane filter and allowed to dry for 30 minutes under vacuum plus another 2 hours without vacuum. The SWNT cake was then delaminated from the filter to obtain a BP (HiPco BP). Four BPs per each fabrication method were produced and each BP was investigated according to the diagram shown in Fig. 2.

Adsorption characterization of BP

Three adsorption parameters were examined: BET surface area, average pore width, and toluene adsorption capacity. A physisorption analyzer (Micromeritics® ASAP 2020, Norcross, GA) was used to obtain surface area and average pore width by N_2 physisorption at 77 K. Samples were desorbed at 100 °C overnight in a lab oven prior to any adsorption parameter measurements. Degassing was conducted with the physisorption analyzer at 300 °C to further remove impurities prior

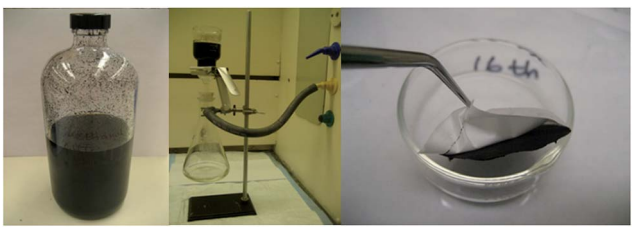

Fig. 1 Typical fabrication procedure: CNT suspension–vacuum filtration–delamination (left to right).

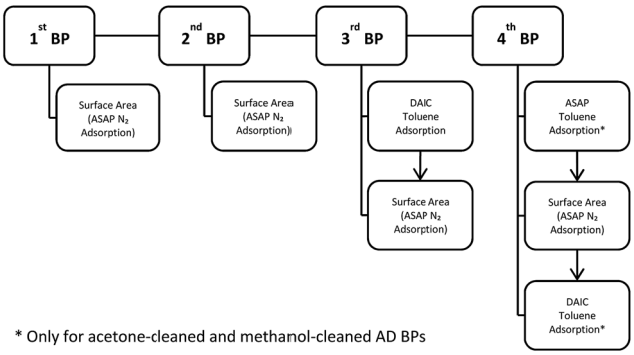

Fig. 2 Diagram of measurements assigned to BPs of each fabrication method.

to analysis. Nitrogen adsorption isotherms were used to determine surface area by BET theory. The average pore width was determined by;

$$d = \frac{4V}{A} \times 10^3 \quad (1)$$

where d is average pore width (nm), assuming cylindrical pores; V is single point total pore volume ($cm^3\ g^{-1}$) at relative pressure ≥ 0.995; A is surface area per unit mass of a sorbent determined by BET theory ($m^2\ g^{-1}$).

Three BPs per fabrication method were analyzed by N_2 physisorption (Fig. 2) with each sample analyzed in triplicate and results averaged.

A diffusive based VOC adsorption isotherm chamber (DAIC) was designed in our lab to obtain toluene adsorption isotherms (30 °C, 303.15 K) and determine adsorption capacity at a given equilibrium concentration (Fig. 3). Toluene flux into the DAIC system was first characterized with a toluene diffusion tube connected to an empty chamber. Toluene concentration in the chamber was continuously monitored with an embedded photo-ionization detector (PID, VOC-TRAQ, Baseline®, Lyons, CO). The mass flux of the toluene was determined by measuring the mass change in time as shown in eqn (2) and (3);

$$F = \sum_{i=1} \frac{\Delta m}{\Delta t} \quad (2)$$

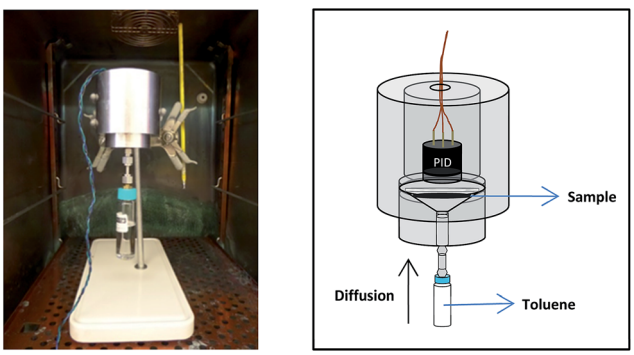

Fig. 3 Diffusive adsorption isotherm chamber (DAIC) system (picture and detailed diagram).

where F is mass flux of the adsorbate (μg s^{-1}); Δm is mass change of adsorbate in the chamber across the time interval (μg); Δt is time interval between measurements (*i.e.*, logging time interval of PID) (s).

$$\Delta m = \left(\frac{\Delta C}{V_m} \times \mathrm{MW}\right) \times V_C \times 10^3 \quad (3)$$

where ΔC is concentration change of the adsorbate in the chamber during the time interval as measured with the embedded PID (ppm); V_m is 25.04, molar volume at the analytical temperature (303.15 K) and pressure (98 992 Pa); MW is molecular weight of adsorbate (92.14 g mol^{-1} for toluene); V_C, is volume of the chamber (47.3×10^{-6} m^3).

The characterization measurements were repeated 6 times and a linear regression equation performed on all 6 trials to obtain an averaged adsorbate mass flux ($R^2 = 0.85$) that accounted for the dynamic concentration gradient as the isotherm progressed;

$$F = -0.000158(C_{eq}) + 0.185214 \quad (4)$$

where F is mass flux of the adsorbate (μg s^{-1}); C_{eq} is equilibrium concentration (ppm).

The mass adsorbed by a sorbent in a given isotherm was calculated using eqn (4) from the concentration in the DAIC over time. Adsorption was allowed to proceed until equilibrium concentration exceeded 800 ppm toluene. Adsorption capacity was expressed as mg (toluene)/g (sorbent).

The third BP from each fabrication method (Fig. 2) was also analyzed for its toluene adsorption capacity using the DAIC system prior to surface area measurement.

To validate the DAIC system, activated carbon sorbent was placed in the DAIC and adsorption allowed to proceed for 2–18.5 hours with gravimetric confirmation of actual mass adsorbed at 5 time intervals (2, 2.3, 4, 5, 18.5 hours). The mean prediction was 87.7 ± 12.3% of actual mass. Additionally two samples (one acetone-cleaned and one methanol-cleaned AD BPs) were sent to Micromeritics® for toluene adsorption analysis by ASAP 2020 physisorption analyzer. Samples were degassed for 960 minutes at 300 °C before analysis and analysis was repeated. Adsorption capacity was calculated by converting the adsorbate gas volume at STP (averaged data obtained from the physisorption analyses) to toluene mass using;

$$m_{adsorbed} = \frac{V_{Gas\cdot STP} \times P_{STP} \times \mathrm{MW} \times 10^3}{R \times T_{STP}} \quad (5)$$

where $m_{adsorbed}$ is mass adsorbed per gram of sorbent (mg g^{-1}); $V_{Gas\cdot STP}$ is gas volume at STP obtained from the physisorption analysis (cm^3 g^{-1}); P_{STP} is standard pressure (101 325 Pa); MW is molecular weight of toluene (92.14 g mol^{-1}); R is ideal gas constant (8.314 Pa m^3 mol^{-1} K^{-1}); T_{STP} is standard temperature (273.15 K).

After the samples were returned, toluene adsorption and BET surface area were re-analyzed since Micromeritics® conducted a substantially longer degassing time (300 °C, 960 minutes) than was used in our lab (300 °C, 60 minutes).

Mechanical properties of BP

The mechanical properties of the methanol-cleaned AD BP and HiPco BP were examined through dynamic mechanical analyzer (TA Instruments RSA-G2, New Castle, DE). For the test 25 mg of each material were used to fabricate BPs. Tensile strength and Young's modulus (E) were determined from the stress-strain curve obtained through the analyzer.

Results and discussion

BET surface area & pore size

The BET surface area and mean pore diameter are as follows for non-cleaned AD, acetone-cleaned AD, methanol-cleaned AD, and HiPco BPs; 211 ± 61 m^2 g^{-1} (8.2 ± 0.1 nm), 322 ± 38 m^2 g^{-1} (9.7 ± 0.5 nm), 387 ± 16 m^2 g^{-1} (8.8 ± 0.4 nm), and 649 ± 3 m^2 g^{-1} (7.7 ± 0.3 nm), respectively (Table 1). After degassing for 960 minutes at 300 °C, BET surface area and mean pore diameter were as follows; 205 ± 1 m^2 g^{-1} (9.7 ± 0.1 nm), 349 ± 10 m^2 g^{-1} (9.8 ± 0.1 nm), 421 ± 6 m^2 g^{-1} (8.6 ± 0.1 nm), and 611 ± 56 m^2 g^{-1} (7.3 ± 0.3 nm) for non-cleaned AD, acetone-cleaned AD, methanol-cleaned AD, and HiPco BPs, respectively.

In general, adsorption capacity is considered to be proportional to the surface area[18] while pore size distribution along with other parameters (*e.g.*, characteristics of the adsorbates) also plays important roles in adsorption capacity.[19] Overall, HiPco BP had the highest surface area and the smallest pore diameter of the BPs fabricated, regardless of degassing. Among AD BPs, methanol-cleaned BPs had the highest surface area with minimal difference in the average pore width. A long degassing process improved surface area for acetone-cleaned and methanol-cleaned AD BPs while non-cleaned AD BPs and HiPco BPs showed no improvement. For HiPco SWNTs which did not contain surfactants the degassing process did not show improvement. The cleaning process as well as the extended degassing of the AD SWNTs helped remove some impurities and using methanol resulted in slightly more adsorptive material than using acetone. Cinke *et al.* reported 567 m^2 g^{-1} surface area with 7.4 nm average pore diameter of HiPco SWNTs (22 wt% as Fe) and a high increased surface area to 1587 m^2 g^{-1} with decreased average pore width (3.9 nm) after two step purification process consisting of dimethylformamide/ethylene diamine treatment (first step) and HCl treatment and wet air oxidation at 225 °C for 18 h (second step).[20] Yang *et al.* obtained 524 m^2 g^{-1} surface area (3.5 nm average pore diameter) with HiPco SWNTs and observed an increased surface area of 861 m^2 g^{-1} after air oxidation at 350 °C for 30 min followed by HCl washing.[21] With an additional annealing at 600 °C after HF treatment, the surface area of HiPco SWNTs was measured as high as 1555 m^2 g^{-1}.[22] Raw AD SWNTs were measured to have 376 m^2 g^{-1} and HCl treatment increased it to 483 m^2 g^{-1}.[23] Few experimental data on surface area of packed/bundled form of CNTs such as BP has been reported in the literature.[24–26] Sweetman *et al.* fabricated HiPco SWNT BPs through filtration method using macrocyclic ligands (β-cyclodextrin sulphated sodium salt (β-CD), 4-sulfonic calix[6]arene hydrate (C6S), *meso*-tetra(4-sulfonatophenyl)porphyrin dihydrogen chloride (TSP), and phthalocyanine tetrasulfonic acid

Table 1 Surface area (SA) and mean pore diameter (*d*) analysis

	Standard degassing (60 min, 300 °C)		Extended degassing (960 min, 300 °C)	
Fabrication methods	BET SA (m^2 g^{-1})	*d* (nm)	BET SA (m^2 g^{-1})	*d* (nm)
Non-cleaned AD BP	211 ± 61	8.2 ± 0.1	205 ± 1	9.7 ± 0.1
Acetone-cleaned AD BP	322 ± 38	9.7 ± 0.5	349 ± 10	9.8 ± 0.1
Methanol-cleaned AD BP	387 ± 16	8.8 ± 0.4	421 ± 6	8.6 ± 0.1
HiPco BP	649 ± 3	7.7 ± 0.3	611 ± 56	7.3 ± 0.3

(PTS)) for suspension and using water and methanol for washing.[24] Surface area was found to be from 30 to 690 m^2 g^{-1} (2–27 nm mean pore diameter), with BP suspended in β-CD having the highest surface area. The same group further fabricated CVD MWNT BPs through the same fabrication process but with dispersants, including C6S, TSP, and PTS.[25] Surface area was in the range of 180 to 250 m^2 g^{-1} (20–26 nm pore diameter). BP fabricated with C6S showed the highest surface area (250 m^2 g^{-1}) which was however much lower than the previously examined SWNT BP fabricated with the same dispersant (580 m^2 g^{-1}). Li *et al.* performed computational modelling studies on BPs made of (5,5) SWNTs and mean pore size tended to be decreasing from 6.4 to 8.4 nm as the SWNT length increased from 50 to 2000 nm, which is in the same order of magnitude with our studies as well as most available literature.[27,28]

As described above, differences in the surface area of CNT are often found. CNTs are broadly categorized into SWNTs and multi-walled carbon nanotubes (MWNTs)[29] and also depending on the synthesis method each can be further categorized (*e.g.*, CVD, AD, laser ablation, HiPco (only producing SWNTs)),[29–31] which makes a difference in their physical and chemical properties. The exact type of CNT is not always available in the literature, different forms of CNTs (*e.g.* powder, solution, BP, *etc.*) are used, and various BP fabrication methods are employed. Because of these circumstances there has not been an agreement on the magnitude of the surface area for each type of CNTs. In this study, we sought to determine which SWNT BP, AD or HiPco, has better adsorption properties, but our AD SWNTs were already suspended using surfactant in water which could have also contributed to the difference in this study. SWNTs in general are available in a variety of purity levels, but the same purity level is not always available in different types of SWNT. Most purification processes modify the physical and chemical properties of SWNTs by introducing defects in the tube walls and adding functional groups such as –COOH or –OH to the defects and tube ends.[32] Our approach in this study was to maintain the physical/chemical integrity of the SWNT substrates as much as possible by not challenging them with harsh conditions such as high temperature peroxide or acid digestion. We found that suspending CNTs in surfactants can negatively affect the BET surface area which can be corrected to varying degrees with solvent cleaning or extended degassing.

Toluene adsorption capacity

Toluene adsorption isotherms obtained with the DAIC system are shown in Fig. 4. Adsorption capacities were determined at 800 ppm equilibrium concentration and found to be 25, 34, 46 and 106 mg toluene/g BP for non-cleaned AD, acetone-cleaned AD, methanol-cleaned AD and HiPco BPs, respectively. The two samples sent to Micromeritics® for verification of DAIC performance (acetone-cleaned and methanol-cleaned AD BPs) were degassed for a much longer time than was our practice (960 min *vs.* 60 min) and were found to have much greater toluene adsorption capacity, 616 and 768 mg g^{-1}, respectively. When these same samples were re-measured using the DAIC system we found adsorption capacities to be 443 and 518 mg g^{-1} at 800 ppm for acetone-cleaned and methanol-cleaned AD BPs, respectively (Fig. 4).

The toluene adsorption capacities obtained through our DAIC system and the physisorption analyzer were overall similar to each other with differences likely due to two major differences in experimental conditions. Adsorption capacities from the physisorption analyzer were at an equilibrium concentration of 28 500 ppm at 25 °C while results from our DAIC system were from an equilibrium concentration of 800 ppm and 30 °C. At higher concentration and lower temperature adsorption capacity is expected to be larger, as was observed in these results.

Notwithstanding, higher toluene adsorption capacity was observed in materials with higher surface area. Adsorption capacities of the samples treated with extended degassing (300 °C for 960 min) showed greatly improved adsorption capacity (12–13 fold increase over solvent cleaning alone), but only modest increases in BET surface area.

CNTs have been extensively investigated for their adsorption for hydrogen storage[33–35] and more recently, literature has shown the use of CNTs in organic compound adsorption.[14,36,37] Adsorption capacity of AD and HiPco SWNTs were examined with several VOCs and toluene was the greatest followed by methyl ethyl ketone (MEK), hexane, and cyclohexane for both types of SWNTs.[14] HiPco SWNTs exhibited higher adsorption capacity (average 356 mg g^{-1}) than AD SWNTs (average 216 mg g^{-1}) for all VOCs examined. Other organic compounds which have been tested include carbon tetrachloride (CCl_4) with AD SWNTs[36] and hydrocarbons, including ethanol, iso-propanol, cyclohexane, cyclohexene, benzene, and *n*-hexane, with SWNTs (not specified).[37] Due to high flexibility, CNT films (*i.e.*, transparent and conductive films, TCFs) have been extensively investigated for electronic device applications.[16,38–40] SWNT films were successfully optimized in terms of in surface smoothness and sheet resistance as hole-injection electrodes for organic light-emitting diodes (OLEDs).[39] Superior

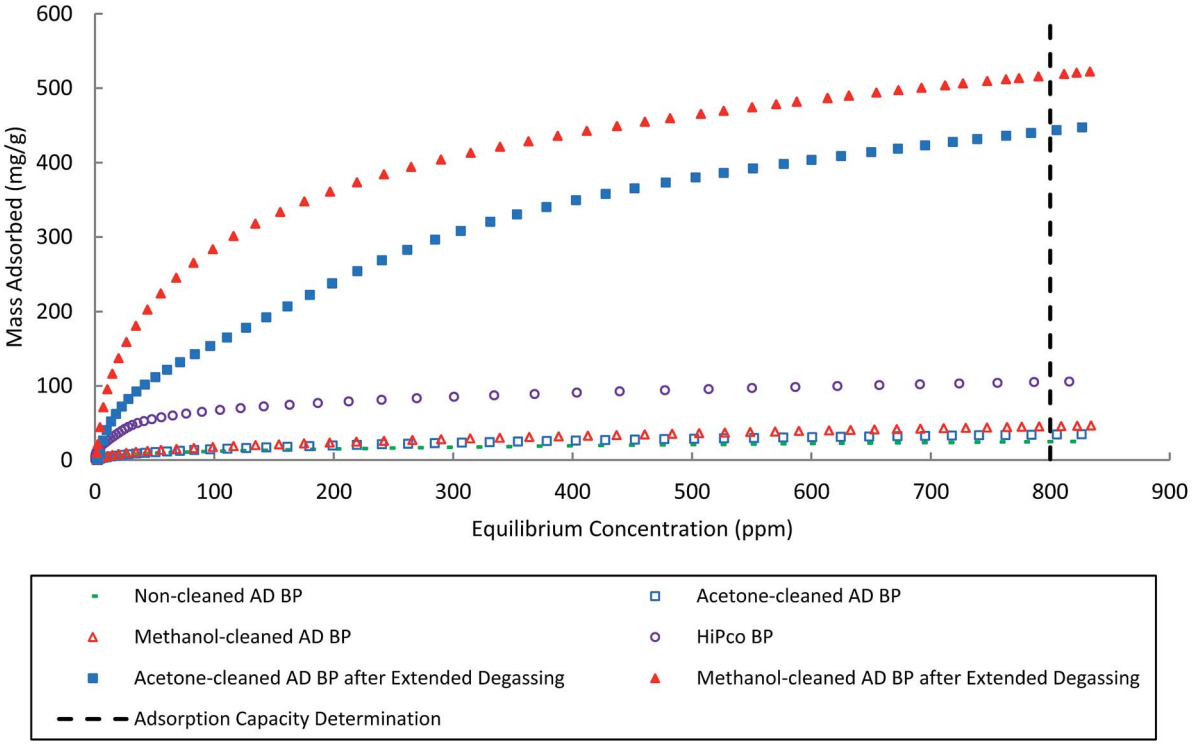

Fig. 4 Toluene adsorption isotherms obtained with DAIC system at 30 °C.

transmittance spectrum of a SWNT film indicated broad applicability in photonic devices.[16] Gas-, bio-sensor and analytical technology is another promising field of CNT film/BP application.[38,41–44] Thin-film transistors constructed from SWNTs were tested with dimethyl methylphosphonate and they were able to detect sub-ppb concentration levels.[41] HiPco SWNT BP was examined as an organic preconcentrator and significant affinity to the tested vapors (toluene, methyl ethyl ketone, and dimethyl methylphosphonate) was observed when thermally desorbed.[43] CVD CNT film deposited in a capillary tube showed high adsorption and fast desorption with high-resolution separation of toluene and hexane.[44] CNT film/BP has also been studied in the water purification and filtration applications.[25,45,46] MWNT BP successfully removed trace organic contaminants in solution and dispersants used to fabricate BP played an important role in the removal efficiency.[25] Most adsorption studies of organic compounds as well as inorganics, however, have been performed in solution mainly for water treatment application with CNT powder.[47,48] Adsorption and desorption characteristics of BP as well as CNT powder using other organic compounds need to be explored further.

Mechanical properties of BP

Methanol-cleaned AD BP and HiPco BP had tensile strength of 59 and 8 MPa and Young's modulus (E) of 11.4 and 1.3 GPa, respectively.

The superior mechanical properties of the methanol-cleaned AD BP could result from parameters like type of CNTs and fabrication procedure (surfactant/solvent, cleaning, *etc.*) and as shown in this study literature reports a somewhat wide range of data.[25,49–52] Zhang *et al.* used BPs fabricated with 100 mg HiPco SWNTs in nitric acid dispersion and the highest acid-concentrated (10 M) BP showed the highest tensile strength and E; 74 MPa and 5.0 GPa, respectively.[51] Sweetman *et al.* also tested HiPco SWNT BPs fabricated using different dispersants (β-CD, C6S, TSP, and PTS).[24] The measured tensile strength was from 6 to 18 MPa, and E was from 0.6 to 2.0 GPa, with PTS the second highest in tensile strength (15 MPa) and the highest in E (2.0 GPa). In a further study, the group examined CVD MWNT BP fabricated with dispersants including C6S, TSP, and PTS.[25] Tensile strength was from 2.5 to 13 MPa and E was from 0.3 to 1.2 GPa, with PTS suspended BP the highest in both properties. Malik *et al.* performed a tensile test for laser ablation SWNT BPs and obtained 10 to 24 MPa, depending on the purification procedure.[52] Computational studies on E have found to be comparable with experimental results.[27,53] (5,5) SWNT BPs with different tube lengths (50–2000 nm) showed E ranging from 0.1 to 0.3 GPa; the shortest having the highest E.[27] Cranford *et al.* modelled (5,5) SWNT BP and reported 0.2–1.4 GPa, E increasing by decreasing porosity.[53] In fact, BPs used in our study for the mechanical test were fabricated with only half mass of the original BPs used in adsorption experiments and the mechanical properties of those BPs are expected to be higher than the obtained data due to increased thickness. Surfactant or solvent effect on mechanical strength/flexibility also has to be further addressed.

Conclusions

We fabricated structurally sturdy BPs through vacuum filtration method for PTD application. The solvent cleaning process

increased BET surface area and decreased average pore diameter for AD BPs. We have observed that the extended high temperature degassing increased the surface area and toluene adsorption capacity of AD BPs, suggesting that the cleaning process did not completely remove surfactant residues. Adsorption capacity increased with increasing surface area of BPs but toluene capacities were much more increased considering the relatively modest increase in surface area after extended degassing. AD BPs will need heat treatment to improve their adsorption properties. Overall, HiPco BP had the best adsorption properties (*i.e.*, surface area, average pore width, and toluene adsorption capacity) as well as a simpler fabrication process compared with AD BPs, indicating suitability for VOC passive sampling and analysis by PTD.

Acknowledgements

This study was supported by the R21 Grant (#1R21OH010373) from National Institute for Occupational Safety and Health (NIOSH). Its contents are solely responsibility of the authors and do not necessarily represent the official views of NIOSH.

References

1 R. Pristas, *Am. Ind. Hyg. Assoc. J.*, 1994, **55**, 841.
2 T. Shih-Wei and S. S. Que Hee, *AIHAJ*, 2000, **61**, 808–814.
3 C. E. Williams, P. N. Pintauro and R. J. Rando, *Am. Ind. Hyg. Assoc. J.*, 1995, **56**, 1074–1082.
4 A. Berlin, R. H. Brown, K. Leichnitz, B. Miller, K. J. Saunders and B. Striefler, *Appl. Ind. Hyg.*, 1988, **3**, R-2–R-6.
5 W. F. Martin, J. M. Lippitt and T. G. Prothero, *Hazardous Waste Handbook for Health and Safety*, Butterworth Publishers, 1987.
6 E. L. Floyd, K. Sapag, J. Oh and C. T. Lungu, *Ann. Occup. Hyg.*, 2014, **58**, 877–888.
7 P. M. Ajayan, M. Terrones, A. De la Guardia, V. Huc, N. Grobert, B. Q. Wei, H. Lezec, G. Ramanath and T. W. Ebbesen, *Science*, 2002, **296**, 705.
8 K. Mizuno, J. Ishii, H. Kishida, Y. Hayamizu, S. Yasuda, D. N. Futaba, M. Yumura and K. Hata, *Proc. Natl. Acad. Sci. U. S. A.*, 2009, **106**, 6044–6047.
9 E. Pop, D. Mann, Q. Wang, K. Goodson and H. Dai, *Nano Lett.*, 2006, **6**, 96–100.
10 A. N. Volkov and L. V. Zhigilei, *Appl. Phys. Lett.*, 2012, **101**, 043113.
11 R. R. Bacsa, C. Laurent, A. Peigney, W. S. Bacsa, T. Vaugien and A. Rousset, *Chem. Phys. Lett.*, 2000, **323**, 566–571.
12 H. Sone, B. Fugetsu, T. Tsukada and M. Endo, *Talanta*, 2008, **74**, 1265–1270.
13 M. Jahangiri, S. J. Shahtaheri, J. Adl, A. Rashidi, H. Kakooei, A. R. Forushani, M. R. Ganjali and A. Ghorbanali, *Fresenius Environ. Bull.*, 2011, **20**, 1036–1045.
14 S. Agnihotri, M. J. Rood and M. Rostam-Abadi, *Carbon*, 2005, **43**, 2379–2388.
15 Z. Shi, X. Chen, X. Wang, T. Zhang and J. Jin, *Adv. Funct. Mater.*, 2011, **21**, 4358–4363.
16 Z. Wu, Z. Chen, X. Du, J. M. Logan, J. Sippel, M. Nikolou, K. Kamaras, J. R. Reynolds, D. B. Tanner, A. F. Hebard and A. G. Rinzler, *Science*, 2004, **305**, 1273–1276.
17 NanoIntegris, How to Create CNT Thin Films with NanoIntegris CNTs in Aqueous Solution, http://www.nanointegris.com/en/downloads, accessed November 10th, 2015.
18 H. Demiral, T. Demiral, B. Karabacakoğlu and F. Tümsek, *Chem. Eng. Res. Des.*, 2011, **89**, 206–213.
19 T. Dobre, O. C. Paîrvulescu, G. Iavorschi, M. Stroescu and A. Stoica, *Ind. Eng. Chem. Res.*, 2014, **53**, 3622–3628.
20 M. Cinke, J. Li, B. Chen, A. Cassell, L. Delzeit, J. Han and M. Meyyappan, *Chem. Phys. Lett.*, 2002, **365**, 69–74.
21 C. M. Yang, K. Kaneko, M. Yudasaka and S. Iijima, *Nano Lett.*, 2002, **2**, 385–388.
22 L. Lafi, D. Cossement and R. Chahine, *Carbon*, 2005, **43**, 1347–1357.
23 M. Eswaramoorthy, R. Sen and C. N. R. Rao, *Chem. Phys. Lett.*, 1999, **304**, 207–210.
24 L. J. Sweetman, L. Nghiem, I. Chironi, G. Triani, M. In Het Panhuis and S. F. Ralph, *J. Mater. Chem.*, 2012, **22**, 13800–13810.
25 M. H. O. Rashid, S. Q. T. Pham, L. J. Sweetman, L. J. Alcock, A. Wise, L. D. Nghiem, G. Triani, M. in het Panhuis and S. F. Ralph, *J. Membr. Sci.*, 2014, **456**, 175–184.
26 H. Muramatsu, T. Hayashi, Y. A. Kim, D. Shimamoto, Y. J. Kim, K. Tantrakarn, M. Endo, M. Terrones and M. S. Dresselhaus, *Chem. Phys. Lett.*, 2005, **414**, 444–448.
27 Y. Li and M. Kröger, *Carbon*, 2012, **50**, 1793–1806.
28 Y. Li and M. Kröger, *Appl. Phys. Lett.*, 2012, **100**, 021907.
29 A. Aqel, K. M. M. A. El-Nour, R. A. A. Ammar and A. Al-Warthan, *Arabian J. Chem.*, 2012, **5**, 1–23.
30 J. I. M. M. A. Rafique, *J. Encapsulation Adsorpt. Sci.*, 2011, 29–34, DOI: 10.4236/jeas.2011.12004.
31 H. Dai, *Surf. Sci.*, 2002, **500**, 218–241.
32 M. E. Itkis, D. E. Perea, S. Niyogi, S. M. Rickard, M. A. Hamon, H. Hu, B. Zhao and R. C. Haddon, *Nano Lett.*, 2003, **3**, 309–314.
33 C. Liu, Y. Y. Fan, M. Liu, H. T. Cong, H. M. Cheng and M. S. Dresselhaus, *Science*, 1999, **286**, 1127–1129.
34 A. C. Dillon, K. M. Jones, T. A. Bekkedahl, C. H. Kiang, D. S. Bethune and M. J. Heben, *Nature*, 1997, **386**, 377–379.
35 Y. Ye, C. C. Ahn, C. Witham, B. Fultz, J. Liu, A. G. Rinzler, D. Colbert, K. A. Smith and R. E. Smalley, *Appl. Phys. Lett.*, 1999, **74**, 2307–2309.
36 M. R. Babaa, N. Dupont-Pavlovsky, E. McRae and K. Masenelli-Varlot, *Carbon*, 2004, **42**, 1549–1554.
37 E. W. Bittner, M. R. Smith and B. C. Bockrath, *Carbon*, 2003, **41**, 1231–1239.
38 Q. Cao and J. A. Rogers, *Adv. Mater.*, 2009, **21**, 29–53.
39 D. Zhang, K. Ryu, X. Liu, E. Polikarpov, J. Ly, M. E. Tompson and C. Zhou, *Nano Lett.*, 2006, **6**, 1880–1886.
40 S. Azoz, A. L. Exarhos, A. Marquez, L. M. Gilbertson, S. Nejati, J. J. Cha, J. B. Zimmerman, J. M. Kikkawa and L. D. Pfefferle, *Langmuir*, 2015, **31**, 1155–1163.
41 J. P. Novak, E. S. Snow, E. J. Houser, D. Park, J. L. Stepnowski and R. A. McGill, *Appl. Phys. Lett.*, 2003, **83**, 4026–4028.

42 A. S. Brady-Estévez, S. Kang and M. Elimelech, *Small*, 2008, **4**, 481–484.
43 F. Zheng, D. L. Baldwin, L. S. Fifield, N. C. Anheier, C. L. Aardahl and J. W. Grate, *Anal. Chem.*, 2006, **78**, 2442–2446.
44 C. Saridara, R. Brukh, Z. Iqbal and S. Mitra, *Anal. Chem.*, 2005, **77**, 1183–1187.
45 K. Sears, L. Dumée, J. Schütz, M. She, C. Huynh, S. Hawkins, M. Duke and S. Gray, *Materials*, 2010, **3**, 127–149.
46 M. Yu, H. H. Funke, J. L. Falconer and R. D. Noble, *Nano Lett.*, 2009, **9**, 225–229.
47 W. Chen, L. Duan and D. Zhu, *Environ. Sci. Technol.*, 2007, **41**, 8295–8300.
48 S. B. Fagan, A. G. Souza Filho, J. O. G. Lima, J. Mendes Filho, O. P. Ferreira, I. O. Mazali, O. L. Alves and M. S. Dresselhaus, *Nano Lett.*, 2004, **4**, 1285–1288.
49 M. M. Zaeri, S. Ziaei-Rad, A. Vahedi and F. Karimzadeh, *Carbon*, 2010, **48**, 3916–3930.
50 G. Xu, Q. Zhang, W. Zhou, J. Huang and F. Wei, *Appl. Phys. A: Mater. Sci. Process.*, 2008, **92**, 531–539.
51 X. Zhang, T. V. Sreekumar, T. Liu and S. Kumar, *J. Phys. Chem. B*, 2004, **108**, 16435–16440.
52 S. Malik, H. Rösner, F. Hennrich, A. Böttcher, M. M. Kappes, T. Beck and M. Auhorn, *Phys. Chem. Chem. Phys.*, 2004, **6**, 3540–3544.
53 S. W. Cranford and M. J. Buehler, *Nanotechnology*, 2010, **21**, 265706.